

Matrix isolated Co atoms: excitation, emission and the photochemical $\text{Co} + \text{H}_2 \rightarrow \text{CoH}_2$ reaction

RONALD L. RUBINOVITZ*, THOMAS A. CELLUCCI† and EUGENE R. NIXON

Department of Chemistry and Laboratory for Research on the Structure of Matter, University of Pennsylvania, Philadelphia, PA 19104, U.S.A.

Abstract—The $a^4P \leftrightarrow a^4F$ transitions in the $12\,000\text{--}14\,000\text{ cm}^{-1}$ region for Co atoms isolated in Ne, Ar and Kr matrices have been explored by excitation and emission measurements. In Ar and Kr, but not in Ne, there is evidence of matrix splitting of the $a^4P_{5/2}$ level. Irradiation in this red region of Ar and Kr matrices containing Co and H_2 (HD, D_2) leads to the formation of the metal dihydride. Rates of the photochemical reaction have been measured at 12K as a function of laser irradiation and show distinct isotope dependence. I.R. vibrational intensities place a lower limit of about 160° for the HCoH valence angle.

INTRODUCTION

Cobalt atoms isolated in inert gas matrices display a very rich emission spectrum [1] throughout the range $11\,400\text{--}27\,400\text{ cm}^{-1}$. Most of the observed emissions correspond to electric dipole forbidden transitions for the gaseous atom but many of them appear as sharp intense lines in the matrix spectrum. The only previous report on matrix-isolated Co atoms is that by MANN and BROIDA [2] who investigated the absorption spectrum in the $25\,000\text{--}45\,000\text{ cm}^{-1}$ ultraviolet region, and thus there is little to compare between emission and absorption results. It may be noted that several studies have been made of complexes of Co atoms in inert gas matrices [3, 4].

In this paper we concentrate on the excitation and emission in the $a^4P \leftrightarrow a^4F$ region around $12\,000\text{--}14\,000\text{ cm}^{-1}$ for Co atoms in Ne, Ar, and Kr matrices. Figure 1 illustrates the lowest lying energy levels of the gaseous atom and in greater detail the a^4P and a^4F multiplets [5]. We also describe an investigation of the photochemical reaction $\text{Co} + \text{H}_2 \rightarrow \text{CoH}_2$, produced by irradiating matrices containing Co atoms and H_2 molecules with laser light in this same spectral region. The results of the Co reaction are compared with an earlier study with Fe atoms [6].

EXPERIMENTAL

Matrices were prepared in either Air Products Displex or Heli-Tran cryostats, using high purity Ne, Ar, Kr, H_2 , D_2 , and HD gases and Co atoms obtained by resistively heating high purity cobalt wire to about 1300K, where the equilibrium vapor pressure of the metal is approximately 10^{-6} torr. Matrix deposition periods varied from 1 to $3\frac{1}{2}$ h but in all cases the estimated gas/Co atom ratio was about 10^4 . Radiation sources included Ar^+ and Kr^+ lasers and a tunable dye laser with Exciton dyes: Coumarin 540, Rhodamine 110, Rhodamine 6G, and LDS-698. Emission and excitation spectra were recorded on a Spex Ramacomp system with $1\text{--}2\text{ cm}^{-1}$ resolution and the i.r. spectra on an IBM/97 FTIR.

*Present address: Naval Research Laboratory, Washington DC 20375, U.S.A.

†Present address: Shell Development Company, Houston, TX 77001, U.S.A.

RESULTS AND DISCUSSION

(i) Matrix-isolated Co atoms

Emission spectra in the $a^4P \rightarrow a^4F$ region for Co atoms in Ar matrices are presented in Figs 2 and 3, each spectrum excited by a different laser frequency. The observed emissions are summarized in Table 1. In general, three series of bands can be identified: a sharp series at $13\,781$, $12\,966$, $12\,375$, and $11\,972\text{ cm}^{-1}$; a second sharp series at $13\,732$, $12\,914$, $12\,323$, and $11\,922$; and a series of broader bands at $13\,666$, $12\,848$, $12\,263$, and $11\,855$. In each case, the spacings clearly show these transitions as terminating in the ground state quartet. The two series of sharp lines originate at levels at $13\,781$ and $13\,732\text{ cm}^{-1}$ [labelled $(\gamma) 4P_{5/2}$ and $(\alpha) 4P_{5/2}$ in Table 1] and are uniformly shifted by -14 or -66 cm^{-1} from the $4P_{5/2} \rightarrow 4F_{9/2, 7/2, 5/2, 3/2}$ transitions of the gaseous atom. From their shapes and frequencies [7], the broad emissions are assigned as phonon side bands of the ZPL transitions originating

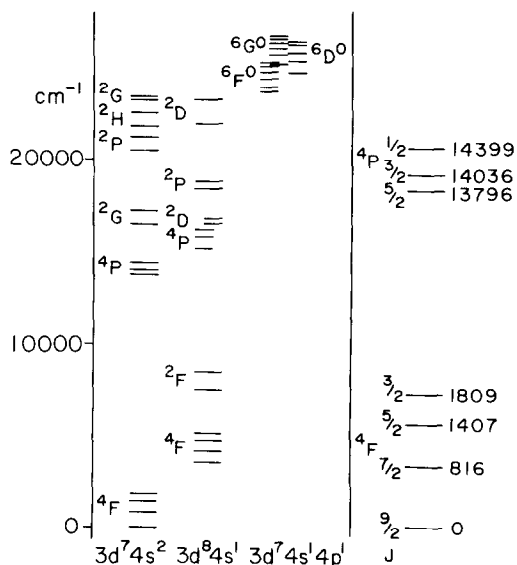


Fig. 1. Diagram of lowest-lying energy levels of gaseous Co atom. On right, the a^4F and a^4P multiplets are shown on expanded scale.

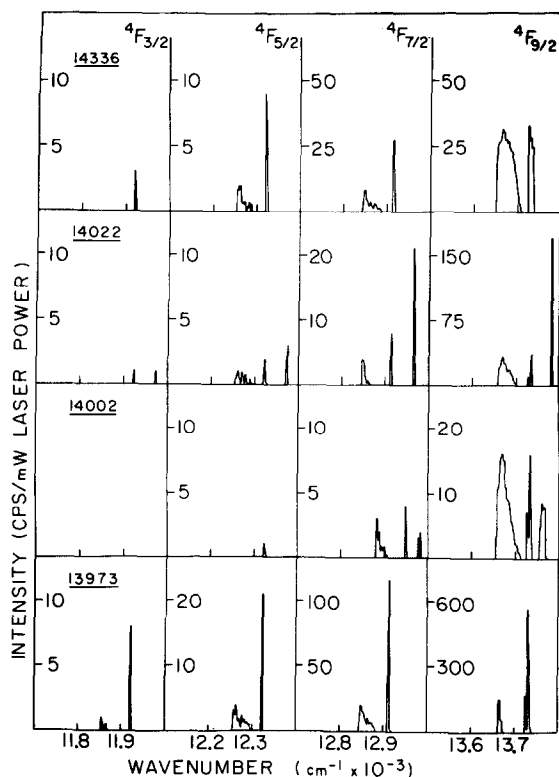


Fig. 2. Emission spectra in the $a^4P_{5/2} \rightarrow a^4F$ region of Co atoms in Ar matrix as excited by laser frequencies underlined. The matrices with Ar/Co = 10^4 were unannealed and spectra were recorded at 25K.

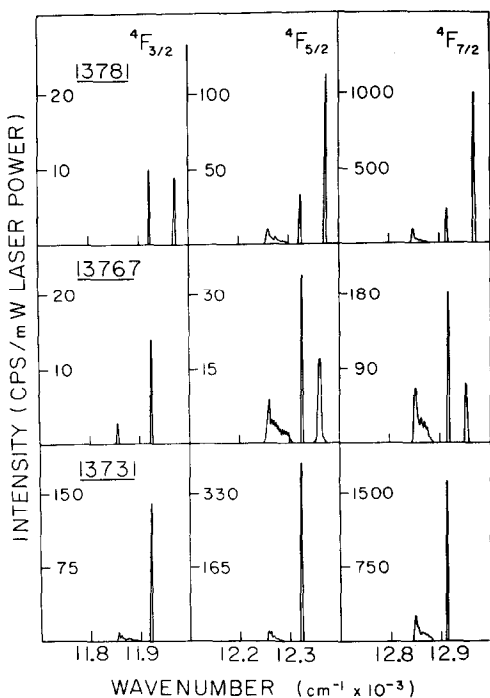


Fig. 3. Emission in the $a^4P_{5/2} \rightarrow a^4F$ region run at 25K for matrix with Ar/Co = 10^4 . The matrix was annealed twice at 43K for a few min. The laser excitations are underlined.

at the (α) $^4P_{5/2}$ level. Finally in the cases of the 14002 and 13767 cm^{-1} excitations, 2 or 3 members of a series of sharp lines appear at 13759, 12950, 12360, and 11960 cm^{-1} . In Table 1, 13759 cm^{-1} is labelled as (β) $^4P_{5/2}$.

The emission spectra suggest that in Ar matrices, the $^4P_{5/2}$ level of the Co atom has possibly three components and that with suitable excitations, transitions can be observed from each component. For confirmation of this splitting, we examined the excitation spectrum over the 4P region (Fig. 4). A strong sharp absorption peak appears at 13731 cm^{-1} , corresponding to (α) $^4P_{5/2}$, and on the high frequency side a weaker absorption spanning the range 13740–13820 cm^{-1} with its maximum at about 13775 cm^{-1} . This latter absorption covers both the (γ) and (β) $^4P_{5/2}$ levels.

In the $^4P_{3/2}$ and $^4P_{1/2}$ regions, the excitation spectrum displays similar patterns with strong though somewhat broader absorptions peaking at about 13975 and 14338 cm^{-1} . The $^4P_{3/2}$ peak appears to have two weak absorptions on the high frequency side. It should be noted that while atoms can be pumped into the $^4P_{3/2}$ and $^4P_{1/2}$ states, the only emission observed unambiguously originates from the $^4P_{5/2}$ levels to which the higher energy states relax. The lifetimes of the (α) $^4P_{5/2}$ and (γ) $^4P_{5/2}$ levels have been measured as about 1200 and 820 μs , respectively [8]; presumably the lifetimes of the $^4P_{3/2}$ and $^4P_{1/2}$ states are much shorter because of phonon-assisted relaxation to $^4P_{5/2}$ and perhaps to other states as well. The weaker absorptions on the high frequency side of the (α) $^4P_{5/2}$, $3/2$, $1/2 \leftarrow ^4F_{9/2}$ transitions in Fig. 4 would appear more likely to be phonon sidebands than components of the 4P states. The only questionable point in this interpretation involves the spacing between the ZPL and the maximum in the phonon sideband. In the excitation spectrum the phonon sideband maximum lies 44 cm^{-1} above the (α) $^4P_{5/2} \leftarrow ^4F_{9/2}$ in the Ar matrix (Fig. 4) and 47 cm^{-1} above in the case of the Kr matrix. In the (α) $^4P_{5/2} \rightarrow ^4F_{9/2}$ emission, on the other hand, the separations between ZPL's and phonon sideband maxima are 61 cm^{-1} in Ar and 50 cm^{-1} in Kr, values more consistent with the phonon densities of states in the rare gas solids.

Both emission and excitation spectra of Co atoms in Kr matrices are remarkably similar to those in Ar matrices, as is illustrated in Fig. 5 and Table 1 for the case of emission. In Kr, however, there is no indication of the (β) $^4P_{5/2}$ level, only the (α) and (γ) components. Figure 5 and Table 1 also compare results of emission spectra in Ne matrices and here only a single component of the $^4P_{5/2}$ level is evident.

Emission results indicate clearly that the $^4P_{5/2}$ state has at least two components, (α) and (γ) , in both Ar and Kr matrices but the excitation spectra fail to provide any convincing corroboration of this splitting.

The possibility of multiple sites for Co atoms in Ar and Kr matrices comes immediately to mind as an explanation for the components of $^4P_{5/2}$ observed in

emission. Cases of multiple site trapping of metal atoms in Ar and Kr have been established. For example, Ni atoms [9, 10] in Ar can exist in two sites: (I) Ni atoms which have the same electronic ground state 3F_4 as the gaseous atom and (II) Ni atoms with 3D_3 ground state. Magnetic circular dichroism studies of Fe atoms in Ar [11] show the presence of two major matrix sites. The aforementioned site effects for Ni and Fe atoms lead to energy level shifts of hundreds of cm^{-1} . In our present experiments with Co atoms, annealing procedures did not change the spectra in any noticeable way and so we are inclined to discount multiple site trapping as the cause of the 49 cm^{-1} separation of the (α) and (γ) components of $^4P_{5/2}$ but we cannot rule it out.

Alternative explanations for the observed splittings include static crystal field and/or dynamic coupling effects. It has been suggested that Fe atoms [8, 11] can occupy substitutional sites in solid argon. If Co atoms

occupied such sites, the octahedral (O_h) field would split the $^4P_{5/2}$ level into $E_{3/2g}$ and $G_{3/2g}$ components but on the basis of the results for Fe atoms in Ar [8] it seems most unlikely that the resulting splitting of the J degeneracy could be as large as the 49 cm^{-1} separation of (α) and (γ) $^4P_{5/2}$.

Splittings of this magnitude have been reported in earlier studies of Fe in Ar [13] in which the a^3P_3 and a^5P_2 states of the atom are each split into two (main) components separated by 37 cm^{-1} . Similar results occur with Ni atoms in Ar [9] for which each of the four states, $a^3D_{3,2,1}$ and a^1D_2 , appear as two components split by $29\text{--}34\text{ cm}^{-1}$. It is interesting to note that each of these particular Fe and Ni states correspond to $3d^n4s^1$ electron configurations. Multiple site splitting can be quite definitely ruled out in these cases since numerous other low lying states of the two atoms, $a^5D_{4,3,2,1,0}$ and a^3P_2 of Fe and $a^3F_{4,3,2}$, b^1D_2 , and $a^3P_{2,1}$ of Ni, all of which come from $3d^{n-1}4s^2$

Table 1. Laser induced emissions from Co atoms isolated in inert gas matrices*

Laser freq.	Matrix peak	Intensity CPS/mW	Ar matrix		Gas to matrix shift (cm^{-1})
				Assignment	
14336	13727	34	(α) $^4P_{5/2}$	$\rightarrow ^4F_{9/2}$	-69
	12913	27		$\rightarrow ^4F_{7/2}$	-67
	12323	9		$\rightarrow ^4F_{5/2}$	-66
	11922	3		$\rightarrow ^4F_{3/2}$	-65
	13666	33	(α) $^4P_{5/2}$	$\rightarrow ^4F_{9/2}$ psb	(-130)
	12848	8		$\rightarrow ^4F_{7/2}$ psb	(-132)
	12263	2		$\rightarrow ^4F_{5/2}$ psb	(-126)
14022	13781	170	(γ) $^4P_{5/2}$	$\rightarrow ^4F_{9/2}$	-15
	12966	21		$\rightarrow ^4F_{7/2}$	-14
	12375	3		$\rightarrow ^4F_{5/2}$	-14
	11972	1		$\rightarrow ^4F_{3/2}$	-15
	13732	37	(α) $^4P_{5/2}$	$\rightarrow ^4F_{9/2}$	-64
	12914	8		$\rightarrow ^4F_{7/2}$	-66
	12323	2		$\rightarrow ^4F_{5/2}$	-66
	11922	1		$\rightarrow ^4F_{3/2}$	-65
	13669	34	(α) $^4P_{5/2}$	$\rightarrow ^4F_{9/2}$ psb	(-127)
	12848	4		$\rightarrow ^4F_{7/2}$ psb	(-132)
	12271	1		$\rightarrow ^4F_{5/2}$ psb	(-118)
14002	13759	9	(β) $^4P_{5/2}$	$\rightarrow ^4F_{9/2}$	-37
	12947	2		$\rightarrow ^4F_{7/2}$	-33
	13732	16	(α) $^4P_{5/2}$	$\rightarrow ^4F_{9/2}$	-64
	12914	4		$\rightarrow ^4F_{7/2}$	-66
	12324	1		$\rightarrow ^4F_{5/2}$	-65
	13669	16	(α) $^4P_{5/2}$	$\rightarrow ^4F_{9/2}$ psb	(-127)
	12848	3		$\rightarrow ^4F_{7/2}$ psb	(-132)
13973	13730	571	(α) $^4P_{5/2}$	$\rightarrow ^4F_{9/2}$	-66
	12912	125		$\rightarrow ^4F_{7/2}$	-68
	12322	21		$\rightarrow ^4F_{5/2}$	-67
	11921	8		$\rightarrow ^4F_{3/2}$	-66
	13664	150	(α) $^4P_{5/2}$	$\rightarrow ^4F_{9/2}$ psb	(-132)
	12847	21		$\rightarrow ^4F_{7/2}$ psb	(-133)
	12261	4		$\rightarrow ^4F_{5/2}$ psb	(-128)
	11855	1		$\rightarrow ^4F_{3/2}$ psb	(-132)
13781	12966	998	(γ) $^4P_{5/2}$	$\rightarrow ^4F_{7/2}$	-14
	12375	112		$\rightarrow ^4F_{5/2}$	-14
	11972	9		$\rightarrow ^4F_{3/2}$	-15
	12914	236	(α) $^4P_{5/2}$	$\rightarrow ^4F_{7/2}$	-66
	12323	33		$\rightarrow ^4F_{5/2}$	-66
	11922	10		$\rightarrow ^4F_{3/2}$	-65
	12848	104	(α) $^4P_{5/2}$	$\rightarrow ^4F_{7/2}$ psb	(-132)
	12260	10		$\rightarrow ^4F_{5/2}$ psb	(-129)

Table 1. (Contd.)

Laser freq.	Matrix peak	Intensity CPS/mW	Ar matrix	
			Assignment	Gas to matrix shift (cm ⁻¹)
13767	12950	72	(β) $^4P_{5/2} \rightarrow ^4F_{7/2}$	-30
	12360	10	$\rightarrow ^4F_{5/2}$	-29
	11960	2	$\rightarrow ^4F_{3/2}$	-27
	12914	182	(α) $^4P_{5/2} \rightarrow ^4F_{7/2}$	-66
	12324	34	$\rightarrow ^4F_{5/2}$	-65
	11923	14	$\rightarrow ^4F_{3/2}$	-64
	12849	75	(α) $^4P_{5/2} \rightarrow ^4F_{7/2}$ psb	(-131)
	12261	9	$\rightarrow ^4F_{5/2}$ psb	(-128)
	11856	3	$\rightarrow ^4F_{3/2}$ psb	(-131)
13731	12913	1618	(α) $^4P_{5/2} \rightarrow ^4F_{7/2}$	-67
	12323	397	$\rightarrow ^4F_{5/2}$	-66
	11922	141	$\rightarrow ^4F_{3/2}$	-65
	12848	248	(α) $^4P_{5/2} \rightarrow ^4F_{7/2}$ psb	(-132)
	12260	24	$\rightarrow ^4F_{5/2}$ psb	(-129)
	11856	4	$\rightarrow ^4F_{3/2}$ psb	(-131)
13783	12965	424	Kr matrix	
	12376	11	(γ) $^4P_{5/2} \rightarrow ^4F_{7/2}$	-15
	11974	1	$\rightarrow ^4F_{5/2}$	-13
	12908	177	(α) $^4P_{5/2} \rightarrow ^4F_{7/2}$	-72
	12318	25	$\rightarrow ^4F_{5/2}$	-71
	11917	9	$\rightarrow ^4F_{3/2}$	-70
	12856	274	(α) $^4P_{5/2} \rightarrow ^4F_{7/2}$ psb	(-124)
	12269	25	$\rightarrow ^4F_{5/2}$ psb	(-120)
	11866	5	$\rightarrow ^4F_{3/2}$ psb	(-121)
13788	12956	110	Ne matrix	
	12367	13	$^4P_{5/2} \rightarrow ^4F_{7/2}$	-24
	11964	1	$\rightarrow ^4F_{5/2}$	-22
			$\rightarrow ^4F_{3/2}$	-23

* psb = phonon side band.

configurations, show no measurable splittings at all. The splittings in the Fe and Ni cases appear to be independent of the J values for the levels and hence of the symmetries of the components produced by an octahedral crystal field and so it was concluded that Jahn-Teller effects could not be the dominant cause of the splittings. We proposed [8] that for the Fe and Ni levels arising from $3d^n-14s^1$ the 30–40 cm⁻¹ splittings might be associated with the unpaired 4s electron and suggested a simple molecular orbital picture of an octahedral $M(\text{Ar})_{12}$ exciplex molecule in which occupation of the a_{1g} m.o. of the molecule by the single 4s metal electron gives rise to the requisite energy differences of 30–40 cm⁻¹ between different distributions of the 3d metal electrons in the t_{2g} and e_g m.o.'s.

This simple model is not applicable to the splitting in the $a^4P_{5/2}$ level of the Co atom since that level arises primarily from the $3d^74s^2$ configuration. We shall return to this point in the latter part of the paper.

(ii) $\text{Co} + \text{H}_2 \rightleftharpoons \text{CoH}_2$

Fairly detailed studies of the photo-induced reaction between Fe atoms and H₂ molecules to yield the metal dihydride in inert gas matrices have appeared in the literature [6, 12]. This section describes an analogous investigation of the reaction of Co atoms.

Addition of a few percent H₂ to an Ar matrix containing a low concentration of Co atoms does not change the appearance of the Co emission spectrum, nor does it alter in any significant way the excitation

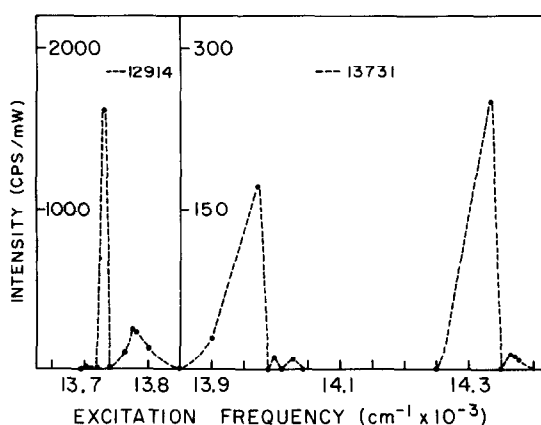


Fig. 4. Excitation spectrum of Co atoms in Ar matrix at 25K with Ar/Co = 10⁴. The matrix was annealed for two 5 min periods at 43K. In left panel, emission monitored by measuring intensity of (α) $a^4P_{5/2} \rightarrow a^4F_{7/2}$ line at 12914 cm⁻¹ and in right panel, the intensity of the (α) $^4P_{5/2} \rightarrow a^4F_{9/2}$ line at 13731 cm⁻¹ was monitored. Experimental points are given by the circles.

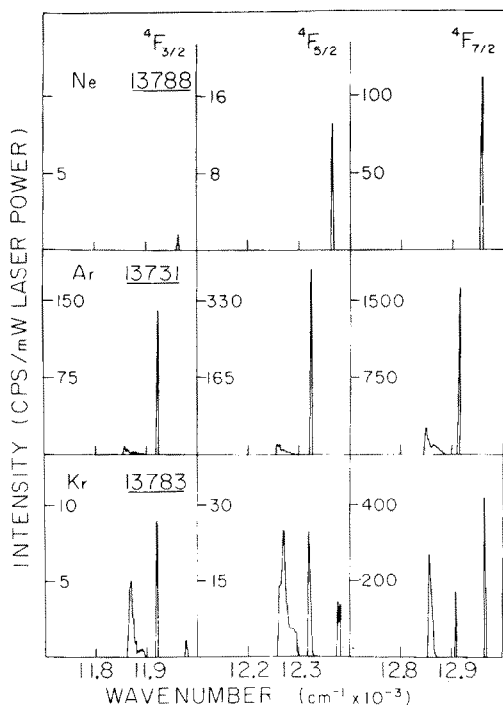


Fig. 5. Emission spectra of Co atoms in the $4P_{5/2} \rightarrow 4F_{7/2}$ region in matrices with $M/Co = 10^4$. Ne matrix, unannealed, run at 5.5K; Ar matrix, annealed twice at 43K, run at 25K; Kr matrix, annealed for 5 min at 43K, run at 25K.

spectrum (upper part of Fig. 6) in the region of concern in this work. The i.r. absorption spectrum in three ranges of interest is shown at the bottom of Fig. 7 for a matrix, with $Co/H_2/Ar$ in the ratios 1/75/2500, deposited and recorded at 12K. Figures 8 and 9 show the spectra for corresponding matrices with D_2 and HD. The 1575–1675 cm^{-1} regions in all three spectra are essentially identical with absorption bands due to the matrix-isolated water which we were unable to avoid. The strongest line at 1624 cm^{-1} is identified as the $1_0 \leftarrow 0_0$ transition of the ν_2 band of H_2O and by the same arguments used in the case of the Fe atom study [6], we conclude that our typical matrix contained at most 4

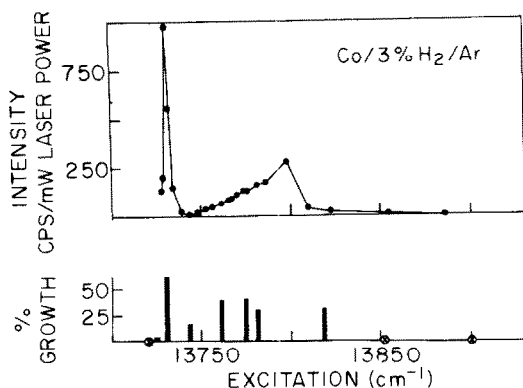


Fig. 6. Top: excitation spectrum of Co atoms by monitoring intensity of the $(\alpha) 4P_{5/2} \rightarrow 4F_{7/2}$ line at 12914 cm^{-1} in a matrix with composition $Co/H_2/Ar = 1/75/2500$ at 12K. Bottom: Graph of data from Table 3.

$\times 10^{-4}$ mmol of H_2O or a Co/H_2O ratio about 10/1. No material effect on the nature of the $Co + H_2$ reaction is expected from this low a concentration of H_2O in the matrix.

Besides the water peaks in the 1575–1675 cm^{-1} region, each of the freshly deposited matrices (bottom spectra in Figs 7–9) exhibits peaks at 1564 and 257 cm^{-1} with intensities proportional to those of the H_2O lines. In a study of Ar matrices containing H_2O along with various metal atoms, HAUGE *et al.* [4] assigned an absorption band at 1564 cm^{-1} to the bending mode of the H_2O molecule in a complex $Co(H_2O)$. Our band at 1564 cm^{-1} is so assigned and because of the parallel intensity behavior, we believe our 257 cm^{-1} band is due to the same complex, possibly the $Co \dots OH_2$ stretching mode. The corresponding band in the $Fe(H_2O)$ case [6] was observed at 270 cm^{-1} .

The middle spectra in Figs 7–9 are for the matrices after 2 h of irradiation at 13781 cm^{-1} . In each case the 1564 and 257 cm^{-1} peaks remain unchanged but new bands appear: 1685 cm^{-1} and a very weak peak at 380 cm^{-1} in the H_2 case; a very weak line at 1223 cm^{-1} with D_2 ; weak lines at 1734, 1245, and 343 cm^{-1} with HD.

The effects of a final irradiation of the matrices with u.v. light are shown in the top spectra in Figs 7–9. In all three instances, this treatment resulted in the bleaching of the $Co(H_2O)$ bands at 1564 and 257 cm^{-1} . On the other hand, the 1685 and 380 cm^{-1} lines in the H_2 spectrum increased in intensity, as did the 1223 cm^{-1} band in D_2 and the 1734, 1245, and 343 cm^{-1} bands with HD. These absorptions are assigned to the Co dihydrides as indicated in Table 2. Observation of a single stretching mode (the asymmetric one) for both CoH_2 and CoD_2 leads to the conclusion that the valence angle is large. On the assumption that the intensity of the unobserved symmetric stretching mode for CoH_2 is no greater than the noise level in the 1720–1680 cm^{-1} region of the spectrum, application of the intensity ratio [6]

$$I_{sym}/I_{asym} = \frac{\cos^2(\alpha/2)}{\sin^2(\alpha/2)} \frac{M_{Co} + 2M_H}{M_{Co} + 2M_H} \quad (1)$$

leads to a minimum value of about 160° for $\alpha < HCoH$. A similar treatment of the vibrational frequencies of $HFeH$ led to a lower limit of about 170° for the valence angle.

The final feature in the i.r. spectra to be discussed is the band at 1791 cm^{-1} which appeared upon u.v. irradiation of the matrices containing H_2 (Fig. 7) and D_2 (Fig. 8). We believe that it corresponds to the 1785 cm^{-1} band reported by HAUGE *et al.* [4] and attributed to the $Co-H$ stretching mode of an insertion product $H-Co-OH$ formed in the photolysis of a $Co/H_2O/Ar$ matrix. The 6 cm^{-1} discrepancy between our frequencies is however unexplained. This peak at 1791 cm^{-1} is barely evident in the HD spectrum (Fig. 9) but it is clear from the spectra that the HD matrix contained less H_2O than those of H_2 and D_2 .

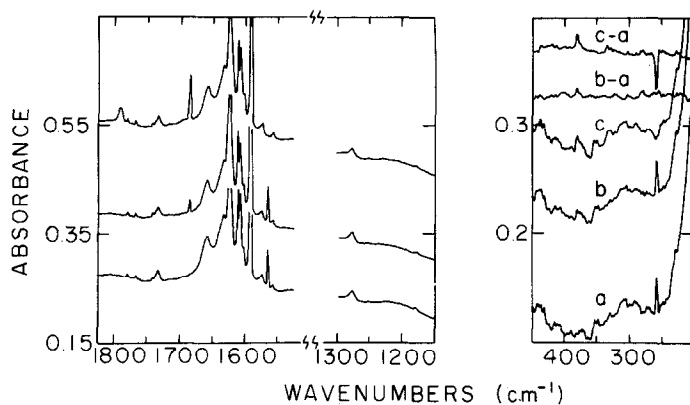


Fig. 7. I.R. spectra of matrix at 12K with mole ratio $\text{Co}/\text{H}_2/\text{Ar} = 1/75/2500$. Bottom: freshly deposited matrix; middle: same matrix after 2 h irradiation with $7 \text{ mW}/\text{cm}^2$ of $13\,781 \text{ cm}^{-1}$ laser light; top: matrix after additional 1.5 h irradiation with $7 \text{ mW}/\text{cm}^2$ of u.v. lines of Ar^+ laser. Some difference spectra are plotted at top right to accentuate the 257 and 380 cm^{-1} bands.

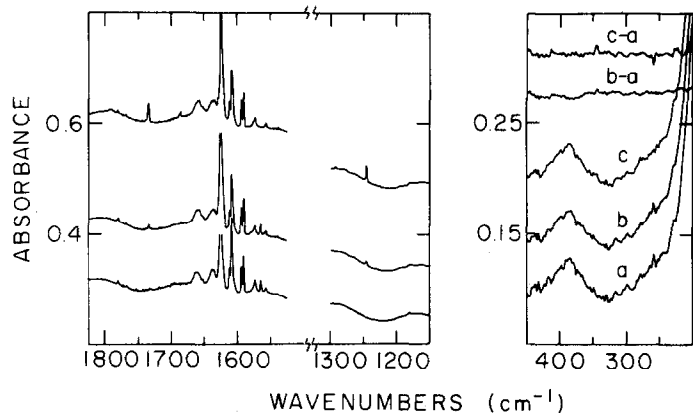


Fig. 8. Same as Fig. 7 except for matrix with $\text{Co}/\text{D}_2/\text{Ar} = 1/75/2500$.

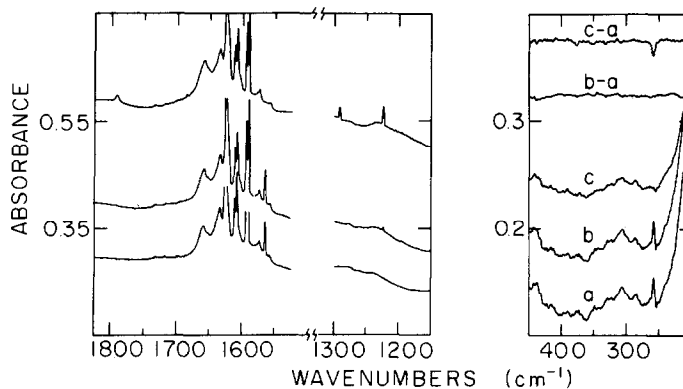


Fig. 9. Same as Fig. 7 except for matrix with $\text{Co}/\text{HD}/\text{Ar} = 1/75/2500$.

The state selectivity of the $\text{Co} + \text{H}_2$ reaction is illustrated in Table 3 and in the bottom portion of Fig. 6, in which the bars represent the percentage of the final (or total) concentration of CoH_2 after a standard irradiation of the matrix by $7 \text{ mW}/\text{cm}^2$ of the laser excitation frequency. Of the excitations examined, the

most effective in the photochemical reaction are the Ar^+ u.v. lines in the $28\,488\text{--}29\,976 \text{ cm}^{-1}$ range. It is not known what specific atomic states in the matrix are pumped by these lines but the $c^2\text{D}(d^9)$ states as well as the $d^7s^1p^1$ multiplets $z^4\text{F}^o$, $z^4\text{G}^o$ and $z^4\text{D}^o$ of the gaseous atom [5] all lie in this range. In the

Table 2. Vibrational frequencies (cm^{-1}) of Co and Fe* dihydrides in inert gas matrices

	CoH ₂		CoD ₂		CoHD	
	Ar	Kr	Ar	Kr	Ar	Kr
Antisym str.	1685	1647	1223	1215	1734	1722
Sym. str.	not obs.	not obs.	not obs.	not obs.	1245	1237
Bend	380	not obs.	not obs.	not obs.	343	
		FeH ₂		FeD ₂		FeHD
		Ar		Ar		Ar
Antisym str.		1661		1205		1691
Sym. str.		not obs.		not obs.		1215
Bend		335		235		301

*Fe data from Ref. [6].

13 720–14 385 cm^{-1} region the only excitation which produced a measurable amount of CoH₂ under our experimental conditions was in the vicinity of the $^4\text{P}_{5/2}$ levels, the most effective being at the (α) $^4\text{P}_{5/2}$ component at 13 731 cm^{-1} .

A series of experiments was designed to measure the rate of the Co + H₂ reaction. In each case the rate of formation is expressed in terms of the ratio I/I_f , where I is the intensity of the i.r. band at 1685 cm^{-1} for CoH₂ (or the band at 1223 cm^{-1} for CoD₂) after a given period of irradiation of the matrix with visible light, and I_f is the final (or total) intensity of that band achieved by a subsequent 15 min of u.v. irradiation. It was first established that the rate is independent of the concentration of H₂ over the range of 1–3%. Next it was shown by varying the laser intensity from 1 to

3 mW/cm² that the reaction is first order in photon flux for the first 180 min of irradiation. Data for a somewhat greater laser intensity of 7 mW/cm² are shown in Fig. 10, in which first order reactions would yield straight lines. First order rate constants calculated from the initial slopes (over the first 30 min) of the curves are listed in Table 4.

While excitation either by the Ar⁺ u.v. lines or by irradiation in the red region near a $^4\text{P}_{5/2}$ results in the combination of Co with H₂, blue light causes decomposition of the dihydride back to Co and H₂. Data for the decomposition caused by the 22 002 cm^{-1} line of the Ar⁺ laser are given in Fig. 11 and first order rate constants derived from the data are listed in Table 4. This deep blue radiation was found to be effective in decomposing FeH₂ as well [6] and in that case OZIN and McCAFFREY [12] proposed that the FeH₂ is pumped into an electronic state having antibonding character in the FeH bonds and bonding between the H atoms so that dissociation into Fe and H₂ occurs.

There are distinct isotope effects in the matrices at 12K on both the rates of formation and dissociation of Co dihydrides. In Ar, CoH₂ forms 4 times faster than CoD₂ and in Kr, the rate is 50 times greater. Decomposition rates of CoH₂ are also faster than for CoD₂ by factors of 2.5 in Ar and 2.6 in Kr. These results indicate a small activation barrier to the dihydride formation, a smaller barrier to dissociation, and an essential independence of the latter process on the particular matrix environment.

(iii) Conclusions

The inference drawn from the infrared spectrum that the valence angle of CoH₂ in Ar is at least 160° is not inconsistent with the potential energy surfaces for CoH₂ as calculated by SIEGBAHN *et al.* [14]. For the (gas phase) ground state, their results give a linear $^4\Phi_g$ structure with CoH bonds of sp hybrid character and length 3.09 a.u. Dissociation of CoH₂ into Co (^4F) and H₂ is a symmetry forbidden reaction so the process has a relatively high barrier of about 45 kcal mol⁻¹ (15 750 cm^{-1}). According to Table 3, irradiation of the matrix over the range 13 725–13 818 cm^{-1} leads to the Co + H₂ → CoH₂ reaction with the maximum rate occurring at 13 731 cm^{-1} , the frequency of the (α)

Table 3. Frequency dependence of relative rates of formation of CoH₂ in Co/H₂/Ar and Co/H₂/Kr = 1/75/2500 matrices at 12K. %CoH₂ is given in terms of intensity of 1685 cm^{-1} absorption line after a period of 2 h irradiation with 7 mW/cm² laser line relative to final intensity of 1685 cm^{-1} line resulting from subsequent irradiation for 15 min. with 7 mW/cm² of u.v. lines of Ar⁺ laser

Laser freq.	Ar		Kr	
	Laser freq.	% CoH ₂	Laser freq.	% CoH ₂
13720		0	13774	35
725		4	27488	100
731		62	28458/482	100
744		17	29976	100
761		40		
775		41		
781		31		
818		31		
851		0		
900		0		
967		0		
973		0		
14002		0		
022		0		
200		0		
336		0		
365		0		
385		0		
27488		100		
28458/482		100		
29976		100		

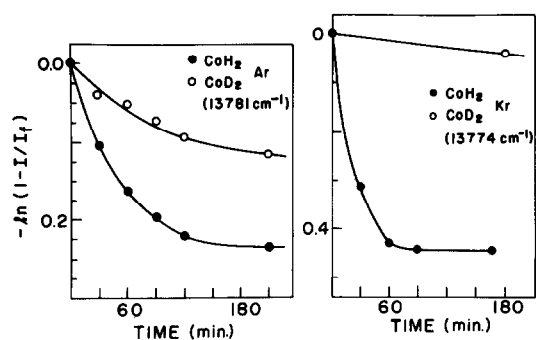


Fig. 10. Time dependence of the formation of CoH_2 and CoD_2 in Ar and Kr matrices at 12K as result of irradiation of the matrices by 7 mW/cm^2 of either 13781 or 13774 cm^{-1} laser light. I are the absorbances of the 1685 cm^{-1} band of CoH_2 and the 1223 cm^{-1} band of CoD_2 in Ar and correspondingly the 1647 and 1215 cm^{-1} bands in Kr. I_f represents the total absorbances of those bands after a final irradiation with Ar^+ u.v. lines. First order reactions should yield straight lines.

Table 4. First order rate constants ($\text{min}^{-1} \times 10^4$) for CoH_2 and CoD_2 formation and decomposition in Ar and Kr matrices from initial slopes in Figs 10 and 11

	Ar matrix		Kr matrix	
	Form.	Decomp.	Form.	Decomp.
CoH_2	35	1050	100	1680
CoD_2	9	400	2	634

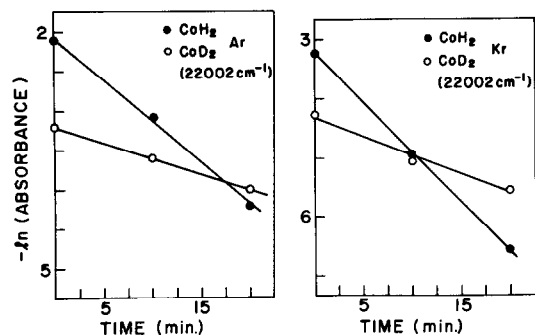


Fig. 11. Time dependence of dissociation of CoH_2 and CoD_2 in Ar and Kr matrices at 12K as result of irradiation of matrices with 7 mW/cm^2 of 22002 cm^{-1} laser light. Absorbances are for 1685 and 1647 cm^{-1} bands of CoH_2 in Ar and Kr, respectively, and for corresponding 1223 and 1215 cm^{-1} bands of CoD_2 .

$^4\text{P}_{5/2} \leftarrow ^4\text{F}_{9/2}$ transition. These energies lie somewhat below the top of the calculated barrier but under our matrix conditions the rate of formation of CoH_2 is rather slow. A typical matrix contained a total of about 10^{18} Co atoms and it is estimated that roughly 5% of these have H_2 neighbors close enough for reaction. From the first order rate constant of $35 \times 10^{-4} \text{ min}^{-1}$ for CoH_2 formation in Ar with 13781 cm^{-1} irradiation, it follows that CoH_2 forms at the rate of 1.75

$\times 10^{14} \text{ mol min}^{-1}$. At the laser power of 7 mW/cm^2 , this represents one CoH_2 mol/ 3.6×10^4 photons of 13781 cm^{-1} radiation. The present work does not provide information on the absorption coefficient of Co atoms at this frequency and thus the rate of CoH_2 formation cannot be compared with the rate of excitation of the Co atoms into the $^4\text{P}_{5/2}$ level.

Matrix irradiation at 29976 cm^{-1} ($85.6 \text{ kcal mol}^{-1}$) at the same laser power level results in CoH_2 production about 11 times faster than with 13781 cm^{-1} light. As stated before, the specific states(s) of the Co atom pumped by the u.v. are not known but the photon energies are well above the reaction barrier.

In the earlier study of the $\text{Fe} + \text{H}_2$ reaction [6], it was shown that irradiation of an Ar matrix at 17524 cm^{-1} ($^5\text{P}_3(d^7s^1) \leftarrow ^5\text{D}_4$) is about 20 times more effective in producing FeH_2 than pumping at 18371 cm^{-1} ($^3\text{P}_2(d^6s^2) \leftarrow ^5\text{D}_4$). It was also demonstrated that the presence of H_2 in the matrix greatly enhances the $^3\text{P}_2 \rightarrow ^5\text{P}_3$ relaxation. There is a close correlation between the emission intensity from the $^5\text{P}_3$ state and the rate of FeH_2 formation, indicating the significance of the role of $^5\text{P}_3(d^7s^1)$ in the reaction. According to the calculations of SIEGBAHN *et al.* [14] the Fe atom has a d^7 configuration in the region of the saddle point of the potential for the dissociation of high spin FeH_2 .

The same calculations [14] suggest that a d^8 configuration is important in the saddle point region for the dissociation of $^4\Phi_g \text{ CoH}_2$. In MOORE'S tables [5] the $a^4\text{P}_{5/2}$ level at 13796 cm^{-1} is assigned to the $3d^74s^2$ configuration and the nearby $b^4\text{P}_{5/2}$ state at 15184 cm^{-1} to $3d^84s^1$. If configuration interaction were to mix these states so that the lower energy one actually contained a significant contribution of $3d^84s^1$, the role of $a^4\text{P}_{5/2}$ in the $\text{Co} + \text{H}_2$ reaction could be rationalized. At the same time, the apparent splitting of the $a^4\text{P}_{5/2}$ state in Ar and Kr would be consistent with those splittings attributed to $d^n s^1$ levels in Fe and Ni atoms.

Acknowledgement—This research was supported by the National Science Foundation under Grant CHE 81-11779. We acknowledge use of the Regional Laser Laboratory at the University of Pennsylvania.

REFERENCES

- [1] T. A. CELLUCCI, Ph.D. thesis, University of Pennsylvania (1984).
- [2] D. M. MANN and H. P. BROIDA, *J. chem. Phys.* **55**, 84 (1971).
- [3] G. A. OZIN and A. VANDER VOET, *Can. J. Chem.* **51**, 637 (1973); L. A. HANLAN, H. HUBER, E. P. KÜNDIG, B. R. MCGARVEY and G. A. OZIN, *J. Am. Chem. Soc.* **97**, 7054 (1975); A. J. LEE HANLAN, G. A. OZIN and W. J. POWER, *Inorg. Chem.* **17**, 3648 (1978).
- [4] R. H. HAUGE, J. W. KAUFFMAN, L. FREDIN and J. L. MARGRAVE, *ACS Symposium Series* 179 (edited by J. L. GOLE and W. C. STWALLEY). Am. Chem. Soc. (1982).
- [5] C. E. MOORE, Atomic Energy Levels, *Natn. Bur. Stand. Circ.* **2**, 467 (1952).
- [6] R. L. RUBINOVITZ and E. R. NIXON, *J. phys. Chem.* **90**, 1944 (1986).

- [7] *Rare Gas Solids*, Vol II, p. 969. (edited by M. L. KLEIN and J. A. VENABLES) Academic, New York (1977).
- [8] T. A. CELLUCCI and E. R. NIXON, *J. phys. Chem.* **89**, 1991 (1985).
- [9] T. A. CELLUCCI and E. R. NIXON, *J. chem. Phys.* **81**, 1174 (1984).
- [10] W. SCHROEDER, R. GRINTER, W. SCHRITTENLACHER, H. H. ROTERMUND and D. M. KOLB, *J. chem. Phys.* **82**, 1623 (1985).
- [11] J. SHAKHS EMAMPOUR, R. PYZALSKI, M. VALA and J.-C. RIVOAL, *J. Phys.* **45**, 953 (1984).
- [12] G. A. OZIN and J. G. McCAFFREY, *J. phys. Chem.* **88**, 645 (1984).
- [13] M. T. MCKENZIE, Jr. and E. R. NIXON, *Chem. Phys.* **75**, 115 (1983).
- [14] P. E. M. SIEGBAHN, M. R. A. BLOMBERG and C. W. BAUSCHLICHER, Jr., *J. chem. Phys.* **81**, 1373 (1984).